

Monitoring of seven industrial anaerobic digesters supplied with biochar

Kerstin Heitkamp

BioEnergie Verbund e.V.

Adriel Latorre-Pérez

Darwin Bioprospecting Excellence

Sven Nefigmann

LUCRAT GmbH

Helena Gimeno-Valero

Darwin Bioprospecting Excellence

Cristina Vilanova

Darwin Bioprospecting Excellence

Efri Jahmad

Robert Boyle Institut e.V.

Christian Abendroth (✉ christian.abendroth@tu-dresden.de)

Robert Boyle Institute <https://orcid.org/0000-0002-3940-9124>

Research

Keywords: Anaerobic digestion, Biochar, DIET, microbial communities

Posted Date: May 13th, 2021

DOI: <https://doi.org/10.21203/rs.3.rs-499198/v1>

License:   This work is licensed under a Creative Commons Attribution 4.0 International License.

[Read Full License](#)

Monitoring of seven industrial anaerobic digesters supplied with biochar

Heitkamp Kerstin^{†1}, Adriel Latorre-Pérez^{†2}, Sven Nefigmann³, Helena Gimeno-Valero²,
Cristina Vilanova², Efri Jahmad⁴, Christian Abendroth^{4,5,*}

[†]Both authors contributed equally to this work

*Corresponding author

¹ BioEnergie Verbund e.V., Jena, Germany

² Darwin Bioprospecting Excellence, S.L. Parc Científic Universitat de Valencia, Paterna,
Valencia, Spain

³ LUCRAT GmbH, Steinfurt, Germany

⁴ Robert Boyle Institut e.V., Jena, Germany

⁵ Technische Universität Dresden, Institute of Waste Management and Circular Economy,
Pirna, Germany

Keywords: Anaerobic digestion, Biochar, DIET, microbial communities

Abstract

Background: Recent research articles indicate that direct interspecies electron transfer (DIET) is an alternative metabolic route for methanogenic archaea that improves microbial methane productivity. It has been shown that multiple conductive materials such as biochar can be supplemented to anaerobic digesters to increase the rate of DIET. However, the industrial applicability, as well as the impact of such supplements on taxonomic profiles, has not been sufficiently assessed to date.

Results: Seven industrial anaerobic digesters were supplemented with biochar for one year. A positive effect was observed for the spectrum of organic acids as the concentration of acetic, propionic, and butyric acid decreased significantly. Quantification of the cofactor F420 using fluorescence microscopy showed a reduction in methanogenic archaea. 16S-rRNA gene amplicon sequencing showed a higher microbial diversity within biochar particles as well as an accumulation of secondary fermenters and halotolerant bacteria. Taxonomic profiles indicate microbial electroactivity, and show the frequent occurrence of *Methanoculleus*, which has not been described in this context before.

Conclusions: Our results shed light on the interplay between biochar particles and microbial communities in anaerobic digesters. Both the microbial diversity and the absolute frequency of the microorganisms involved were significantly changed between sludge samples and biochar particles. This is particularly important against the background of microbial process monitoring. In addition, it could be shown that biochar is suitable for reducing the content of inhibitory, volatile acids on an industrial scale.

1. Background

Anaerobic Digestion is a methane-yielding process carried out by a microbial biocenosis composed of bacteria and methanogenic archaea. Firstly, substrate is hydrolysed by bacteria. Further degradation by acetogenic bacteria leads to the formation of mainly organic acids, alcohols, hydrogen and carbon dioxide. Eventually, the aforementioned metabolites are transformed into acetate, hydrogen and carbon dioxide during acetogenesis. Metabolites produced by acetogenic bacteria are transformed by methanogenic archaea into methane [1]. Methanogenesis is usually divided into three major pathways: acetoclastic-, hydrogenotrophic and methylotrophic methanogenesis [2]. In all three pathways, acetate, format, hydrogen and several methyl compounds (mono-, di- and trimethylamines) serve as electron carriers for a unique kind of respiration that uses carbon dioxide as electron acceptor [3]. If electrons are transported with the aforementioned carriers, this process is also referred to as mediated interspecies electron transfer (MIET). However, more recent articles show that electrons can also be transported by conductive particles, direct cell contact or microbial nanowires. This more direct way of electron transport is known as direct interspecies electron transfer (DIET) [4]. To increase the electroactivity of anaerobic digester microbiomes, multiple researchers have presented the possibility to increase the rate of DIET by adding conductive particles. In the past years, there has been a gold rush in the search for suited supplements. A particularly exotic one has recently been presented based on phenazine crystals [5]. It has been shown that phenazine crystals can form long and needle like conductive structures, which overgrew with methanogenic archaea during the respective experiments.

A recent review by Martins et al. (2018) gives a detailed overview on many substances that have been applied to increase electroactivity, and the most popular ones are magnetite, hematite, granular activated carbon, carbon cloth and biochar [6]. The exact mechanisms of DIET and its impact on anaerobic digester communities is still under investigation. However, the first mechanisms have already been proposed. According to an article by Zhang et al. (2019), DIET contributed to lower hydrogen partial pressures, which in turn lowered the concentration of butyric acid [7].

“*Syntrophie among Prokaryotes*” is described extensively in a review article by Schink and Stams (2006). A wide range of syntrophically degraded substrates are known, among them several amino acids, ethanol, butyrate, propionate, acetate and several aromatic compounds. Many syntrophic reactions release hydrogen [8]. Enzymatic reactions are usually bidirectional [9], and the direction that releases hydrogen is thermodynamically unfavoured for the abovementioned substrates. However, the hydrogen releasing reaction occurs in spite of slightly endergonic reactions. Due to its poor solubility, hydrogen degasses rapidly from aqueous solutions, which prevents a hydrogen consuming backreaction. The syntrophic partner organisms of such reactions contribute to low hydrogen pressures as they consume hydrogen in an exergonic reaction and very fast. Summing up both syntrophic reactions - the hydrogen producing and the hydrogen consuming -, the resulting reaction is exergonic.

As the hydrogen releasing reaction is thermodynamically unfavoured, it is very sensitive to hydrogen pressures. If hydrogen consumption is inhibited, or if hydrogen production is too fast, a slight increase in the hydrogen pressure might take place and inhibit the syntrophic degradation [8]. As conductive particles allow direct electron transport without the need for hydrogen interspecies transfer (HIT), this explains the enhancement in syntrophic butyric acid degradation described by Zhang et al. (2019), as previously mentioned.

Although the basic concept of syntrophy is well understood in anaerobic digestion, there is still much to learn about it. To give here an example of the underlying complexity, a recent study presented a model in which Clostridia, *Syntrophomonas*, *Methanosaeta* and hydrogenotrophic methanogens are intertwined [10]. Hydrolytic clostridia produce fatty acids and acetate, and these fatty acids are further transformed to acetate by the acetogenic bacterium *Syntrophomonas*. Acetate is converted into carbon dioxide and methane by the acetoclastic methanogen *Methanosaeta* (*Methanotrix*) and, together with hydrogen, the produced carbon dioxide can then be converted to methane by hydrogenotrophic methanogens. However, it is also possible for *Methanotrix* to reduce carbon dioxide itself, using a direct inflow of electrons. Using ferrous iron, this inflow of electrons might be generated by *Syntrophomonas* during

the acetogenic degradation of fatty acids [10]. The aforementioned microbial community indicates that direct- and indirect transfers of electrons are microbiologically intertwined. Additionally, it is poorly understood how conductive particles affect taxonomic profiles in anaerobic digesters. In the past few years, several articles have been published which highlight electroactive prokaryotes that are meaningful for anaerobic digesters. Important electroactive bacteria are, for example, the genera *Shewanella* [11] and *Geobacter* [12]. Among archaea, the acetoclastic methanogens *Methanosarcina* and *Methanotherix* appear to be important [6], and a recent study demonstrated that methanogenic archaea can form electrically conductive protein filaments, in particular, the hydrogenotroph methanogen *Methanospirillum hungatei* [13]. Also, it has been recently reported that the *Methanobacterium* strain YSL is able to form syntrophic aggregates with *Geobacter metallireducens* [14]. Altogether, recent information about DIET indicates that electroactivity occurs in a wide range of organisms within anaerobic digester microbiomes. As DIET seems to be a common phenomenon, which additionally allows enhancement of anaerobic digester microbiomes, this topic is of high interest for the biogas industry. However, to our best knowledge, there are no or very scarce studies that investigate the effect of conductive particles on industrial anaerobic digester microbiomes. The present study aims to close this gap. Therefore, seven different industrial digesters were analyzed with F420 fluorescent microscopy upon addition of large amounts of biochar. One digester was investigated in detail based on 16S-rRNA gene amplicon high-throughput sequencing. It has to be highlighted that not only DNA from sludge samples was analyzed, but also from biochar particles that were collected from fresh digestate.

2. Results & Discussion

3.1 Influence of biochar on the spectrum of organic acids

At the beginning of the project, our research consortium was contacted by seven industrial anaerobic digester plants, who were interested in applying biochar as a supplement (as described in material and methods). At first, only BGP2 and BGP6 were in a critical condition

reaching very high concentrations of total volatile fatty acids (TVFAs; 8058.98 mg L⁻¹ of TVFAs for BGP2 and 4983.3 mg L⁻¹ for BGP6). BGP1, BGP2-BGP5 and BG7 had TVFA concentrations lower than 2000 mg L⁻¹.

Although no reliable dataset for the biogas productivity was given, all operators have regularly commissioned suitable service providers for chemical analyses, as described in material and methods. All raw data are provided in the supplementary file S1. Most of the raw data yielded no meaningful interpretation. However, upon biochar supplementation a decrease throughout time of TVFAs was observed for acetic acid, propionic acid and butyric acid (Fig. 1). In general, it was difficult to compare the provided data, as the conditions between BGP1-7 varied strongly. The respective plant operators recorded chemical parameters irregularly, and for some of the plants only analyses for very few time points were provided. To facilitate the interpretation, the concentrations of acetic-, propionic-, and butyric acid were normalized to a value between 0 and 1. VFA concentrations from all plants were treated as one data cloud and a trend was calculated based on the least square's method. The trend was clear and significant for acetic acid and propionic acid (Fig. A and Fig. 1B). For butyric acid, only a slight -but yet significant- decrease was observed (Fig. 1C).

[Figure 1 here]

The observed decrease in acetic, propionic, and butyric acid concentrations is in accordance with existing literature. A recent study at laboratory scale demonstrated that conductive materials help lower the concentrations of propionic and butyric acids, and explained that this phenomenon is due to an increased rate of DIET, which in turn reduced the amount of inhibiting hydrogen [7]. The here presented results confirm the effect of conductive materials on organic acid concentrations and demonstrate this phenomenon for the first time at an industrial scale. The organic loading rate for all digesters is shown in table 1, and all plant operators confirmed that the respective loading rate was maintained throughout the study. Therefore, the reduced concentration of organic acids cannot be explained by a change of loading rate.

3.2 F420-fluorescent microscopy upon biochar addition

Before biochar was applied to BGP1-BGP7, all plant operators provided fresh sludge samples for the analysis of methanogenic archaea based on the cofactor F420. After 9 and 11 months, all plant operators provided further samples for F420 analysis. F420 signals were counted using the ImageJ software (Fig. 2). In general, the detected concentration of methanogenic archaea was in a similar range as in other studies [15, 16]. Interestingly, the number of methanogenic archaea seemed to decrease slightly throughout time upon the addition of biochar. Although the decrease was not observed for all timepoints (BPA1 behaved different) and samples for BGP6 and BGP7 were not accessible during month 11, a two-tailed paired t-test revealed a significant decrease of the archaea number for BGP2, BGP3, BGP5 and BGP6. Although not significant, BGP4 and BGP7 showed a decrease in methanogenic archaea as well (Fig. 2B).

[Figure 2 here]

Regarding methanogenic phenotypes, mainly cocci were observed. In a recent study, conductive particles led to an increase in the ratio of acetoclastic methanogens [10]. Acetoclastic methanogens that are typically involved in anaerobic digestion processes are *Methanothrix* and *Methanosarcina* [17, 18]. However, typical phenotypes for *Methanothrix* (thread-like) or *Methanosarcina* (sarcina-like cluster) were scarcely detected. On average, less than one *Methanosarcina* cluster was detected per picture (Figure 2C). Although this number is very small, it is interesting that all of the plants tested, with the exception of BGP7, showed an increase in the number of *Methanosarcina*-like clusters and some of them were significant. No clear trend was observed for rod-like and thread-like phenotypes (Fig. 2D). As the hydrogenotrophic methanogen *Methanoculleus* (coccus shape) is usually enriched in continuous stirred tank reactors [10], and mainly methanogenic cocci were detected in the

analyzed digesters, our results suggest that *Methanoculleus* was also prevalent in the present study. In the case of BGP1, this assumption was verified by 16S-rRNA gene amplicon high-throughput sequencing (Fig. 5). Under the assumption that supplemented biochar increased the rate of DIET, our results suggest that hydrogenotrophic methanogens could be involved in DIET. In concordance with this hypothesis, recent studies have suggested that DIET is more widespread than previously thought, and that DIET is not only restricted to acetoclastic methanogens. To give some examples: recently, the first methanogen able to produce electrically conductive pili was detected, and identified as the hydrogenotrophic *Methanospirillum hungatei* [19]. Another recent study suggested that the hydrogenotrophic *Methanobacterium* is able to perform DIET [20]. Regarding *Methanoculleus*, several species have been tested in vitro, but were not able to grow in syntrophic co-culture with the typical electrogenic bacterium *Geobacter metallireducens* [21]. Therefore, although the present results suggest that *Methanotherix* might be capable of DIET, further *in vitro* studies must be performed to confirm this result.

3.3 Fluorescence microscopy with grinded biochar particles

The fluorescence microscopy results shown in figure 2 were performed with sludge, with no insight into biochar particles, therefore further experiments were performed focusing on biochar particles. The plant operator of BGP1 provided access to several tons digestate, which left the reactor exactly before the sampling. Two falcon tubes were filled with biochar particles, which were collected directly from the digestate. In a first analysis, biochar particles were grinded to powder and resuspended in 1 ml of PBS buffer per 1 g of powder. Upon inverting, the samples were analyzed using fluorescence microscopy [Fig. 3].

[Figure 3 here]

Although the number of methanogenic archaea was much lower in the grinded biochar powder compared to the fresh sludge (Fig. 3A), grinded biochar particles clearly contained methanogenic archaea (Fig. 3B). Biochar samples which were not inserted into the digesters did not show F420-signals. As previously described for highly viscous sludge from continuous stirred tank reactors [17], very little *Methanosarcina*-like clusters were found, which was also the case in BGP1-BGP7 (Fig. 2C). Still, a few *Methanosarcina* were observed, even in the grinded biochar powder, suggesting that the biochar pores were big enough for such cluster-forming methanogens (Fig. 3C). The majority of the observed methanogens were cocci, suggesting that the same methanogens were present in both the biochar and the sludge.

3.4 Analysis of taxonomic profiles of grinded biochar particles at phylum level

To obtain a more detailed insight into the taxonomic profiles present in the sludge and in the biochar particles from BGP1, 16S-rRNA gene amplicon high-throughput sequencing was performed. The main phyla present in all samples were *Firmicutes* (~69%), *Bacteroidota* (~13%) and Proteobacteria (~4%) (Figure 4).

[Figure 4 here]

The grinded biochar samples displayed a higher –yet not significant- relative abundance of *Bacteroidota* and a lower relative abundance of *Firmicutes* (FDR adjusted p-value < 0.05; DESeq2 test) in comparison to the digester sludge samples. *Firmicutes* are well known degraders of plants and complex carbohydrates [22]. The lower ratio of *Firmicutes* in the biochar samples might indicate that bacteria within biochar particles are rather associated with secondary fermentation (acetogenesis) than with hydrolytic and acidogenic events. Our results also revealed that biochar powder contained higher relative abundances of *Acidobacteria*, *Halanaerobiaeota*, *Halobacterota* and *Proteobacteria*, although only *Acidobacteria* changed significantly. This suggests that biochar particles are subjected to more

stressful conditions: *Acidobacteria* are described as robust and adapted to stressful conditions in soil [23]; *Halanaerobiaeota* and *Halobacterota* are generally known to be associated with high salt contents and their higher abundance might be explained by the adsorptive characteristics of biochar; and *Proteobacteria* are associated with nitrogen- and ammonium metabolism [24] and, therefore, their increased abundance in the biochar might be explained due to precipitation of ammonia within the biochar. Altogether, our results indicate that adsorptive characteristics of biochar particles can lead to locally increased concentrations of salt and other inhibitors, which in turn has a strong impact on the underlying taxonomic profile. It must be noted that the phylum *Chloroflexi* showed a significant higher abundance in the biochar powder (FDR adjusted p-value < 0.05; DESeq2 test). In a previous report, an enrichment of *Chloroflexi* in anaerobic biofilms was described [25]. It has also been reported that *Chloroflexi* can be involved in syntrophic relations [26, 27]. In relation to the aforementioned decrease of Firmicutes, this supports the hypothesis that biochar particles are particularly involved into syntrophic degradation processes. On the other hand, *Cyanobacteria* was overrepresented in the sludge samples (FDR adjusted p-value < 0.05; DESeq2 test). It has to be noted that the sequencing reads assigned to *Cyanobacteria* could correspond partially to chloroplasts, which are an indicator of undegraded plant biomass. 0.3% of the reads represent chloroplasts (PCC-6307). The remaining reads (1.6%), which were assigned as *Cyanobacteria*, are represented by the genus *Cyanobium* (*data not shown*). This phenomenon has been previously reported for a lab-scale reactor, which was fed with fresh grass biomass and were high ratio of *Cyanobacteria* was observed [25].

3.5 Analysis of taxonomic profiles of grinded biochar particles at genus level

The most abundant genera detected in both sets of samples were *Limnochordia* MBA03 (36.46% in biochar samples and 46.08% in sludge), *Proteiniphilum* (13.78% and 7.38%), *Caldicoprobacter* (4.53% and 8.15%) and *Amphibacillus* (2.29% and 4.15%).

[Figure 5 here]

The frequency of *Limnochordia MBA03* is of special interest, since this genus was observed in a cathodic enrichment culture in 2018 [28]. In a recent article, in which 20 biogas plants were compared, this organism was observed together with *Methanosarcina*, and a syntrophic relationship has been suggested between both of them [29]. The fact that *Limnochordia MBA03* occurs both in the biochar particles and in the liquid phase could indicate that the biochar particles can also be used as conductive structures by microorganisms in the liquid phase. At this point, however, it cannot be ruled out that *Limnochordia MBA03* also grows on other conductive structures or even without conductive structures, as this genus was also abundant in anaerobic digesters not treated with conductive particles [29]. Besides *Limnochordia MBA03*, the genus *Proteiniphilum* is another hint for electroactivity as this genus has been described within electroactive consortia [30]. *Proteiniphilum* is known to grow on nitrogen rich substrates (e.g., yeast, peptone). In the case of *Proteiniphilum acetatigenes*, this species is unable to grow on multiple carbohydrates, alcohols and fatty acids [31], suggesting an intense nitrogen metabolism within biochar particles. This might be explained by the fact that poultry manure, known for its high nitrogen content, was among the substrates that were fed into BGP1 (Tab. 1).

Regarding the sludge samples, the ratio of *Proteiniphilum* was much lower in comparison to the biochar samples. On the other hand, the sludge samples displayed much higher ratios for *Caldicoprobacter*, a genus known to grow with high ammonium concentrations [32]. A reason for the shift from *Caldicoprobacter* to *Proteiniphilum* might be a local enrichment of ammonia in the biochar particles, which *Proteiniphilum* might tolerate better than *Caldicoprobacter*. Another explanation could be that nitrogen metabolism was supported by electroactivity in the biochar particles, as it is well known that several amino acids are degraded in syntrophic relations [8]. It has been previously postulated that *Caldicoprobacter* is involved in syntrophic oxidation processes, but this has not yet been brought into connection with electroactivity [33].

Therefore, it could be possible that biochar particles increased the rate of DIET during nitrogen metabolism, which in turn caused a shift from *Caldicoprobacter* to *Proteiniphilum*.

Although bacteria-specific primers were used (as described in material and methods), several archaea were recorded. One methanogen (*Methanoculleus*) was even among the most abundant prokaryotic genera (Fig. 5). The fact the mainly *Methanoculleus* was found is in accordance with above-described microscopic results, where mainly cocci were found. Taking into account that applied biochar particles may increase the rate of DIET, our results suggest that *Methanoculleus* may be involved in DIET. However, since *Methanoculleus* has not been described as capable to perform DIET so far, this needs to be further studied. Interestingly, the relative abundance of *Methanoculleus* was higher in the biochar particles (2.29%) than in the sludge (0.43%), supporting the previous hypothesis that biofilms on biochar particles are more involved in secondary fermentations steps (in syntrophic relation with methanogenesis).

3.6 Microbial diversity on biochar particles is increased

To investigate whether microbial diversity differed between biochar particles and general sludge, the α - and β -diversity of both groups of samples were calculated (Fig. 6). The β -diversity is shown in a principal component analysis (PCoA) and indicates that the microbial communities of sludge samples and powdered biochar are substantially different from each other. Regarding archaea, the biochar samples analyzed in this work did not only display a higher relative abundance of *Methanoculleus* (Fig. 5), but also a higher α -diversity of methanogenic archaea (Fig. 6A). Interestingly, this increased diversity was also observed when considering all prokaryotic genera (Fig. 6B). There are several reasons, which might explain these observations. For example, the porous surface could facilitate biofilm formation, and adsorption might influence the microbial community as well. Due to adsorption, a local enrichment of salt and inhibitors might cause very harsh conditions in the biochar particles, forcing the involved microorganisms to continuously adapt. Although one might expect to obtain a lower diversity under harsh or even extreme conditions, some authors describe high

diversities under extreme conditions. For example, it has been described that numerous alkaline and hypersaline environments show high microbial diversity, and that the adaptive mechanisms under extreme conditions can enable very useful capabilities, such as a “*control of membrane permeability, control of intracellular osmotic balance, and stability of the cell wall, intracellular proteins, and other cellular constituents*” [34].

Based on the aforementioned observations, it is possible to hypothesise that digester sludge provides a large and endless reservoir of microorganisms, that are forced to develop adaptive mechanisms once they come into contact with the respective biochar particles.

The aforementioned assumption that salt and inhibiting compounds are enriched in biochar particles is in agreement with the existing literature. For example, a recent study described that 5 different biochar types, which were evaluated as supplements for anaerobic digestion, retained Fe, Co, Ni and Mn [35]. Also, the potential enrichment of functional microbes has been previously suggested, particularly in respect to the stimulation of the secretion of extracellular polymeric substances (rapid sludge granulation), increased microbial abundance and improvement of DIET [36].

Interestingly, other authors have described an enrichment of *Sporanaerobacter* and *Enterococcus*, *Methanosarcina* [37] and *Methanotherix* [38] on biochar. In the present study, none of these genera were enriched, suggesting that the biochar microbiome is even more complex than previously thought. A reason for this difference might be that the biochar surface and the inner region of the biochar particles can be colonized differently. Although many of the articles discussed in a recent review [36] highlight an enrichment of *Methanosarcinales*, it is also mentioned that these species grow especially on the surface of biochar particles. In contrast, the inner regions might promote the growth cocci such as *Methanoculleus*, which are smaller than the threadlike or cluster forming *Methanosarcinales* [36].

[Figure 6 here]

3. Conclusions

After analyzing the application of biochar in seven industrial anaerobic digesters, a decreasing concentration for butyric, propionic, and acetic acid was observed. Reduction of VFA concentrations might be explained due to an increased rate of DIET, which is in accordance with existing literature. The present study confirms this effect at an industrial scale.

Based on epifluorescent microscopy, a shift in the number of methanogenic archaea was observed, suggesting that there is a decrease in methanogenic cell numbers in sludge and an increase in the respective biochar particles. One of the digesters was analyzed in more detail by comparing the taxonomic profiles in the sludge and in hand-picked biochar particles from fresh digestate. The taxonomic profile in the biochar particles substantially differed from the one observed in the sludge samples, and this profile suggested an increased electroactivity associated to the biochar particles, as well as an increased biodiversity, which should be characterised in depth in future studies.

4. Materials & Methods

4.1 Analyzed digesters & biochar supplementation

Seven German anaerobic digesters plants were supplemented with biochar over a duration of one year. An overview of the respective digester plants is given in Table 1. All digester systems analyzed were industrial continuous stirred tank reactors and it must be noted that several of them were in a problematic state, indicated by high concentrations of acetic acid. All digester systems were supplemented with 1.8 Kg of biochar per t of reactor content (“Carboferm” from the LUCRAT GmbH). The biochar was added stepwise into the digesters over 12 days. Following this, biochar was added to the substrate with ratio of 1.8 kg of biochar per t of substrate.

[Table 1 here]

4.2 Analysis of organic acids

Biogas productivity could not be measured during the experiments. Sporadically, chemical parameters were recorded by the companies T&B – Die Biogasoptimierer GmbH (Tarp, Germany) and WESSLING GmbH (Altenberge, Germany). These companies recorded total solids (TS), volatile solids (VS), content of ammonia (NH₄-N), pH, spectrum of organic acids and the volatile organic acid and buffer capacity ratio (FOS/TAC). Only the content of acetic acid-, propionic- and butyric acid provided useful information for the present study (Fig. 1), and the respective raw data are recorded for each plant (Supplementary File S1).

4.3 Quantifying the cofactor F420

Involved digester plants sent their samples by overnight mail order to the Robert Boyle Institute (Jena, Germany), and samples were analyzed upon receipt. For this, samples were diluted 1:10 with a mounting solution (RotiR-Mount FluorCare, Carl-Roth, Germany), and 3 µL of the diluted sample were pipetted between the cover slip and the slide. An epifluorescent microscope (Axio Lab.A1, Carls Zeiss, Germany) was used to quantify cofactor F420 as an indirect measure of methanogenic archaea load. The methodology was similar to a recent study from Hardegen et al. [15]. Excitation occurred with wavelengths ranging from 400 to 440 nm. Emitted light with wavelengths between 500 nm and 550 nm was collected and analyzed using the ImageJ-Software (400Å~ magnification and 126 ms exposure time). For each sample, 48 pictures were analyzed. In total, samples from three time points were collected: (1) control before adding biochar; (2) after 9 months of supplementation with biochar; and (3) after 11 months of supplementation with biochar.

From all seven digesters plants, one plant provided access for further analysis (BGP1). To get a deeper insight into the taxonomic profile of the anaerobic digester microbiome, samples were taken from the digester liquor, and biochar fragments from fresh digestate were collected manually. Upon the sampling, the digester liquor was analyzed under the microscope as described above. Biochar fragments were grinded and resuspended in PBS buffer (1 g of powdered biochar per 1 ml of PBS). After vortexing, 2 µl of the resuspended biochar powder

was pipetted between the cover slip and the slide. Following this, the cofactor F420 was analyzed as previously described. Additionally to the fluorescent microscopy, liquid samples and biochar fragments were fixed in 50% ethanol for subsequent DNA analysis (16S-rRNA amplicon gene high-throughput sequencing).

4.4 16S-rRNA gen amplicon high-throughput sequencing

Primers 341F (5' CCT AYG GGR BGC ASC AG 3') and 806R (5' GGA CTA CNN GGG TAT CTA AT 3') were used to amplify the V3-V4 region of the 16S rRNA gene for prokaryotes. All PCR reactions were carried out with Phusion® High-Fidelity PCR Master Mix (New England Biolabs). PCR products were mixed at equal density ratios. The pool was then purified with Qiagen Gel Extraction Kit (Qiagen, Germany). Sequencing libraries were generated with NEBNext® Ultra™ DNA Library Prep Kit for Illumina and quantified via Qubit and q-PCR. Finally, the NovaSeq 6000 Sequencing System (2 x 250 bp) was employed for sequencing the samples. All sequence data are stored in the Sequence Read Archive (SRA) of the National Center for Biotechnology Information (NCBI; Bioproject: PRJNA727077).

4.5 Bioinformatic analysis

Raw Illumina sequences were analysed using Qiime2 (v. 2020.8) [39]. Briefly, the quality of the reads was assessed with the Demux plugin, and the sequences were subsequently corrected, trimmed and clustered into amplicon sequence variants (ASVs) via DADA2 [40]. The taxonomy of each sequence variant was assigned employing the classify-Sklearn module from the feature-classifier plugin. SILVA (v. 138) was used as reference database for 16S rRNA alignment [41]. It is worth highlighting that SILVA's nomenclature was used for taxonomy (i.e., Bacteroidota was used instead of Bacteroides). Phyloseq package was employed for analysing the data [42]. All the α -diversity tests were carried out using ASVs and rarefying to the lowest library size (=115,626 seqs). DESeq2 was used for differential abundance analyses [43].

Author's contributions

SN supplied the biogas plants with biochar particles and collected chemical process parameters. CA organized the sampling and designed the work. KH was responsible for fluorescent microscopy. AL, HG CV extracted DNA, organised the sequencing of selected samples and performed statistical analyses. KH, AL and CA prepared the figures. CA, AL and CV wrote the manuscript. All authors have read and approved the final version of the manuscript.

Acknowledgements

We are grateful for funding of the work by the German Ministry of Economic Affairs and Energy (grant numbers 16KN070129 and 005-1907-0285). We are also grateful for funding by the German Ministry for the Environment, Nature Conservation and Nuclear Safety (grant number 16EXI4016A). We are indebted to Kristie Tanner for her technical support and critical review of the manuscript. AL is a recipient of a Doctorado Industrial fellowship from the Spanish Ministerio de Ciencia, Innovación y Universidades (reference DI-17-09613).

Statement on ethics approval and consent

Not applicable

Consent for publication

Not applicable

Availability of data and materials

All sequence data are stored in the Sequence Read Archive (SRA) of the National Center for Biotechnology Information (NCBI; Bioproject: PRJNA727077).

Competing interests

All authors declare that there are no financial and non-financial competing interests.

Funding

The BioEnergie Verbund e.V. received funding from the German Ministry of Economic Affairs and Energy (grant number 16KN070129).

The LUCRAT GmbH and the Robert Boyle Institute e.V. received funding from the German Ministry of Economic Affairs and Energy (grant number 005-1907-0285).

The TU Dresden received funding from the German Ministry for the Environment, Nature Conservation and Nuclear Safety (grant number 16EXI4016A).

Adriel Latorre-Pérez (Darwin Bioprospecting Excellence) is a recipient of a Doctorado Industrial fellowship from the Spanish Ministerio de Ciencia, Innovación y Universidades (reference DI-17-09613).

References

[1] Robles G, Nair RB, Kleinstaub S, Nikolausz M, Horváth IS; Biogas Production: Microbiological Aspects. In: Biogas: Fundamentals, Process and Operation; Biogas, Biofuel and Biorefinery Technologies 6; Tabatabaei M, Ghanavati H, editors. Springer Nature 2018; https://doi.org/10.1007/978-3-319-77335-3_7.

[2] Lambie, S.C., Kelly, W.J., Leahy, S.C., Li, D., Reilly, K., McAllister, T.A., Valle, E.R., Attwood, G.T., Altermann, E.; 2015. The complete genome sequence of the rumen methanogen *Methanosarcina barkeri* CM1. Stand Genomic Sci. 10:57.

- [3] Fenchel, T., King, G.M., Blackburn, T.H.; Chapter 1 - Bacterial Metabolism. In: Bacterial Biogeochemistry (Third Edition), Academic press, 2012. pp 1-34, ISBN 9780124158368.
- [4] Cheng, Q., Douglas, F.C.; 2016. Hardwiring microbes via direct interspecies electron transfer: mechanism and applications. Environ. Sci.: Processes Impacts. 18, 968.
- [5] Beckmann, S., Welte, C., Li, X., et al.; 2016. Novel phenazine crystals enable direct electron transfer to methanogens in anaerobic digestion by redox potential modulation. Energy Environ Sci. 9, 644.
- [6] Martins, G., Salvador, A.F., Pereira, L., Alves, M.M.; 2018. Methane Production and Conductive Materials: A Critical Review. Environ Sci Technol. 52. 10241 – 10253.
- [7] Zhang, M., Ma, Y., Dandan, J., Xueyuan, L., Zhang, J., Zang, L.; 2019. Synergetic promotion of direct interspecies electron transfer for syntrophic metabolism of propionate and butyrate with graphite felt in anaerobic digestion. Bioresour Technol. 287:121373. doi: 10.1016/j.biortech.2019.121373.
- [8] Schink, B., Stams, A.J.M.; 2006. Syntrophism among Prokaryotes. The Prokaryotes / Martin Dworkin (ed.-in-chief) ... ; Vol. 2. New York: Springer, 2006, pp. 309-335.
- [9] Robinsion, P.K.; 2015. Enzymes: principles and biotechnological applications. Essays Biochem. 59, 1-41.
- [10] Zhao, Z., Li, Y., Yu, Q., Zhang, Y.; 2018. Ferroferric oxide triggered possible direct interspecies electron transfer between *Syntrophomonas* and *Methanosaeta* to enhance waste activated sludge anaerobic digestion. Bioresource Technology 250, 79 – 85.

- [11] Brutinel, E.C., Gralnick, J.A.; 2012. Shuttling happens: soluble flavin mediators of extracellular electron transfer in *Shewanella*. *Appl Microbiol Biotechnol.* 93, 41-48.
- [12] Rotaru, A.E., Shrestha, P.M., Liu, F.; 2014. A new model for electron flow during anaerobic digestion: direct interspecies electron transfer to *Methanosaeta* for the reduction of carbon dioxide to methane. *Energy Environ Sci.* 7, 408.
- [13] Walker, J.F., Martz, E., Holmes, D.E., Zhou, Z., Nonnenmann, S.S., Lovely, D.R.; 2019. The Archaeum of *Methanospirillum hungatei* Is Electrically Conductive. *MBio.* pii: e00579-19. doi: 10.1128/mBio.00579-19.
- [14] Zheng, S., Liu, F., Wang, B., Zhang, Y., Lovley, D.R.; 2020. *Methanobacterium* Capable of Direct Interspecies Electron Transfer. *Environ Sci Technol.* 54, 15347-15354.
- [15] Hardegen, J., Latorre-Pérez, A., Vilanova, C., Günther, T., Porcar, M., Luschig, O., Simeonov, C., Abendroth, C.; 2018. Methanogenic community shifts during the transition from sewage mono-digestion to co-digestion of grass biomass. *Bioresource Technology* 265, 275-281.
- [16] Nettmann, E., Bergmann, I., Pramschfuer, S., Mundt, K., Plogsties, V., Herrmann, C., Klocke, M., 2010. Polyphasic analyses of methanogenic archaeal communities in agricultural biogas plants. *Appl. Environ. Microbiol.* 76, 2540–2548.
- [17] Abendroth C., Vilanova C., Günther T., Luschig O., Porcar M., 2015. Eubacteria and Archaea communities in seven mesophile anaerobic digester plants. *Biotechnology for Biofuels* 8:87.

- [18] Sundberg, C., Al-Soud, W.A., Larsson, M., Alm, E., Yekta, S.S., Svensson, B.H., Sørensen, S.J., Karlsson, A., 2013. 454 pyrosequencing analyses of bacterial and archaeal richness in 21 full-scale biogas digesters. *FEMS Microbiol. Ecol.* 85 (3), 612–626.
- [19] Walker, J.F., Martz, E., Holmes, D.E., Zhou, Z., Nonnenmann, S.S., Lovley, D.R.; 2019. The Archaeellum of *Methanospirillum hungatei* Is Electrically Conductive. *MBio*. pii: e00579-19. doi: 10.1128/mBio.00579-19.
- [20] Zheng, S., Liu, F., Wang, B., Zhang, Y., Lovley, D.R.; 2020. *Methanobacterium* Capable of Direct Interspecies Electron Transfer. *Environ Sci Technol.*: <https://doi.org/10.1021/acs.est.0c05525>
- [21] Yee, M.O., Rotaru, A.E., 2020. Extracellular electron uptake in *Methanosarcinales* is independent of multiheme c-type cytochromes. *Sci Rep.* 10: 372.
- [22] Flint, H.J., Scott, K.P., Duncan, S.H., Louis, P., Forano, E., 2012. Microbial degradation of complex carbohydrates in the gut. *Gut microbes.* 3, 289-306.
- [23] Männistö, M.K., Kurhela, E., Tirola, M., Häggblom, M.M., 2013. Acidobacteria dominate the active bacterial communities of Arctic tundra with widely divergent winter-time snow accumulation and soil temperatures. *FEMS Microbiol Ecol.* 84, 47-59.
- [24] Wang, F., Xia, S.Q., Liu, Y., Chen, X.S., Zhang, J., 2007. Community analysis of ammonia and nitrite oxidizers in start-up of aerobic granular sludge reactor. *J Environ Sci.* 19, 996-1002.
- [25] Abendroth, C., Simeonov, C., Peretó, J., Antúnez, O., Gavidia, R., Luschign, O., Porcar, M., 2017. From grass to gas: microbiome dynamics of grass biomass acidification under mesophilic and thermophilic temperatures. *Biotechnology for Biofuels* 10:171.

- [26] Narihiro, T., Nobu, M.K., Kim, N.K., Kamagata, Y., Liu, W.T., 2015. The nexus of syntrophy-associated microbiota in anaerobic digestion revealed by long-term enrichment and community survey. *Environ Microbiol.* 17, 1707-1720.
- [27] Saha, S., Jeon, B.H., Kurade, M.B., Govindwar, S.P., Chatterjee, P.K., Oh, S.E., Roh, H.S., Lee, S.S., 2019. Interspecies microbial nexus facilitated methanation of polysaccharidic wastes. *Bioresour Technol.* 289, 121638.
- [28] Rago, L., Zecchin, S., Marzorati, S., Goglio, A., Cavalca, L., Cristiani, P., Schievano, A.; 2018. A study of microbial communities on terracotta separator and on biocathode of air breathing microbial fuel cells. *Bioelectrochemistry.* 120, 18-26.
- [29] Calusinska, M., Goux, X., Fossépré, M., Muller, E.E.L., Wilmes, P., Delfosse, P.; 2018. A year of monitoring 20 mesophilic full-scale bioreactors reveals the existence of stable but different core microbiomes in bio-waste and wastewater anaerobic digestion systems. *Biotechnol Biofuels.* 11, 196.
- [30] Lesnik, K.L., Cai, W., Liu, H.; 2019. Microbial Community Predicts Functional Stability of Microbial Fuel Cells. *Environ. Sci. Technol.* 54:1.
- [31] Chen, S., Dong, X., 2005. *Proteiniphilum acetatigenes* gen. nov., sp. nov., from a UASB reactor treating brewery wastewater. *Int J Syst Evol Microbiol.* 55:2257-2261.
- [32] Poirier, S., Desmond-Le, Q.E., Madigou, C., Bouchez, T., Chapleur, O.; 2016. Anaerobic digestion of biowaste under extreme ammonia concentration: identification of key microbial phylotypes. *Bioresour Technol.* 207:92–101.

- [33] Jiang, Y., Dennehy, C., Lawlor, P.G., Hu, Z., McCabe, M., Cormican, P., Zhan, X., Gardiner, G.E.; 2019. Exploring the roles of and interactions among microbes in dry co-digestion of food waste and pig manure using highthroughput 16S rRNA gene amplicon sequencing. *Biotechnol Biofuels*. 12:5.
- [34] Mesbah, N.M., Wiegel, J.; 2012. Life under Multiple Extreme Conditions: Diversity and Physiology of the Halophilic Alkalithermophiles. *Appl Environ Microbiol*. 78, 4074-4082.
- [35] Wambugu, C.W., Rene, E.R., van de Vossenberg, J., Dupont, C., van Hullebusch, E.D., 2019. Role of Biochar in Anaerobic Digestion Based Biorefinery for Food Waste. *Front Energy Res*. doi: 10.3389/fenrg.2019.00014.
- [36] Tang, S., Wang, Z., Liu, Z., Zhang, Y., Si, B.; 2020. The Role of Biochar to Enhance Anaerobic Digestion: A Review. *JRM*. 8:9.
- [37] Dang, Y., Holmes, D. E., Zhao, Z., Woodard, T. L., Zhang, Y. et al. (2016). Enhancing anaerobic digestion of complex organic waste with carbon-based conductive materials. *Bioresource Technology*, 220, 516–522. DOI 10.1016/j.biortech.2016.08.114.
- [38] Ren, S., Usman, M., Tsang, D. C. W., Thong, O. S., Angelidaki, I. et al. (2020). Hydrochar-facilitated anaerobic digestion: evidence for direct interspecies electron transfer mediated through surface oxygen-containing functional groups. *Environmental Science & Technology*, 54(9), 5755–5766. DOI 10.1021/acs.est.0c00112.
- [39] Bolyen, E., Rideout, J.R., Dillon, M.R., et al. Reproducible, interactive, scalable and extensible microbiome data science using QIIME 2. *Nat Biotechnol* 2019;**37**:852–7. doi:10.1038/s41587-019-0209-9

[40] Callahan BJ, McMurdie PJ, Rosen MJ, et al. DADA2: High-resolution sample inference from Illumina amplicon data. *Nat Methods* 2016;13:581–3. doi:10.1038/nmeth.3869

[41] Quast C, Pruesse E, Yilmaz P, *et al.* The SILVA ribosomal RNA gene database project: Improved data processing and web-based tools. *Nucleic Acids Res* 2013;41:590–6. doi:10.1093/nar/gks1219

[42] McMurdie PJ, Holmes S. Phyloseq: An R Package for Reproducible Interactive Analysis and Graphics of Microbiome Census Data. *PLoS One* 2013;8. doi:10.1371/journal.pone.0061217

[43] Love MI, Huber W, Anders S. Moderated estimation of fold change and dispersion for RNA-seq data with DESeq2. *Genome Biol* 2014;15:1–21. doi:10.1186/s13059-014-0550-8

Figure and table captions

Table 1: Overview on digester systems: all systems were mesophilic continuous stirred tank reactors (CSTRs).

Figure 1: Evolution of organic acid concentration upon biochar supplementation: after normalization to a value between zero and one, mean values were calculated for all seven digesters (BGP1 – BGP7). Concentrations were recorded over a duration of one year. The significance of the decrease in organics acids was assessed applying a nonparametrical Spearman test.

Figure 2: Quantification of methanogenic archaea before and after supplementation: The cofactor F420 was used to count methanogenic archaea using epifluorescent microscopy. The QQ plot resulting from the Shapiro-Wilk test is shown as an example for the counting of all archaea (A), but it was also carried out for the counting of *Methanosarcina*-like clusters and rod-shaped and thread-like archaea (A). Analysis was performed before biochar was added, and nine and eleven months after supplementation. Each bar shows a mean value of 48 pictures taken from three different slides. (B), *Methanosarcina* like clusters (C), and rod-shaped archaea (D). A two-tailed paired t-test was applied to assess significance.

Figure 3: Methanogenic archaea found in biochar particles: After applying the Shapiro Wilk test (A), a two-tailed paired t-test was used to assess significance for all archaea. Number of methanogenic archaea based on the quantification of cofactor F420 signals (B). Biochar particles from BGP1 were collected from the digestate immediately after it left the digester. Pictures of methanogenic archaea found in biochar particles (C). *Methanosarcina*-like clusters are highlighted with white arrows.

Figure 4: Taxonomic profiles in sludge and biochar from BGP1 at phylum level, obtained through 16S-rRNA gene amplicon high-throughput sequencing. For the sake of simplicity, only the most abundant phyla are shown. Differences in the mean values that are significant are highlighted by yellow stars in the legend. Significances were analyzed using the DESeq2 differential abundance analysis [21] and p-values were < 0.05 .

Figure 5: Taxonomic profiles in sludge and biochar from BGP1 at genus level and obtained through 16S-rRNA gene amplicon high-throughput sequencing. For the sake of simplicity, only the most abundant genera are shown. Differences in the mean values that are significant are highlighted by yellow stars in the legend. Significances were analyzed using the DESeq2 differential abundance analysis [21] and p-values were < 0.05 .

Figure 6: Microbial diversity in biochar particles on genus level: (A) α -diversity of archaea according to richness (Observed) and diversity indices (Shannon and Simpson); (B) α -diversity of all genera according to richness (Observed) and diversity indices (Shannon and Simpson); (C) β -diversity of all genera represented through a Principal Coordinates Analysis.

Supplementary file 1: Recorded raw data for acetic-, propionic-, and butyric acid.

Figures

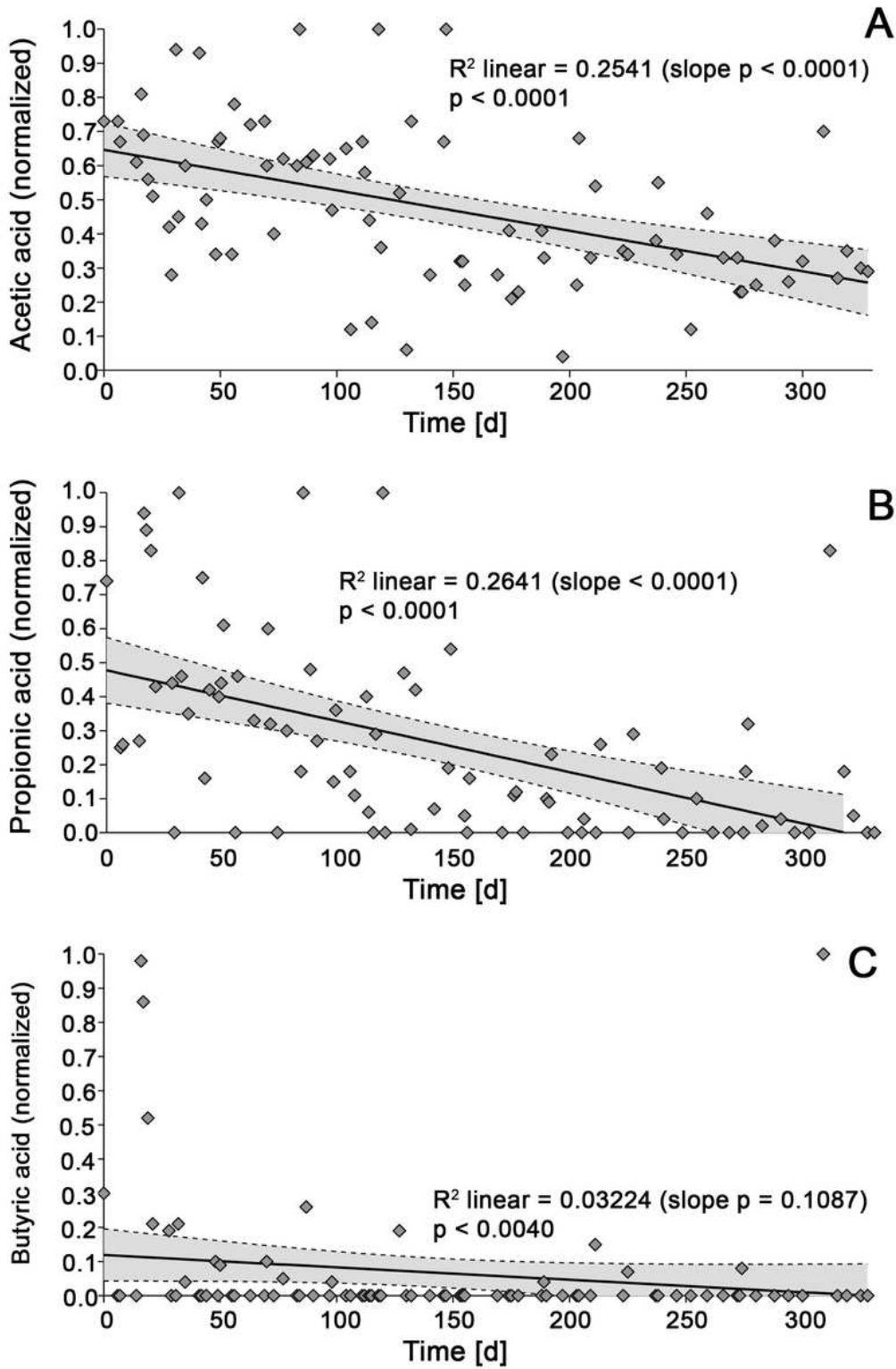


Figure 1

Evolution of organic acid concentration upon biochar supplementation: after normalization to a value between zero and one, mean values were calculated for all seven digesters (BGP1 – BGP7).

Concentrations were recorded over a duration of one year. The significance of the decrease in organics acids was assessed applying a nonparametrical Spearman test.

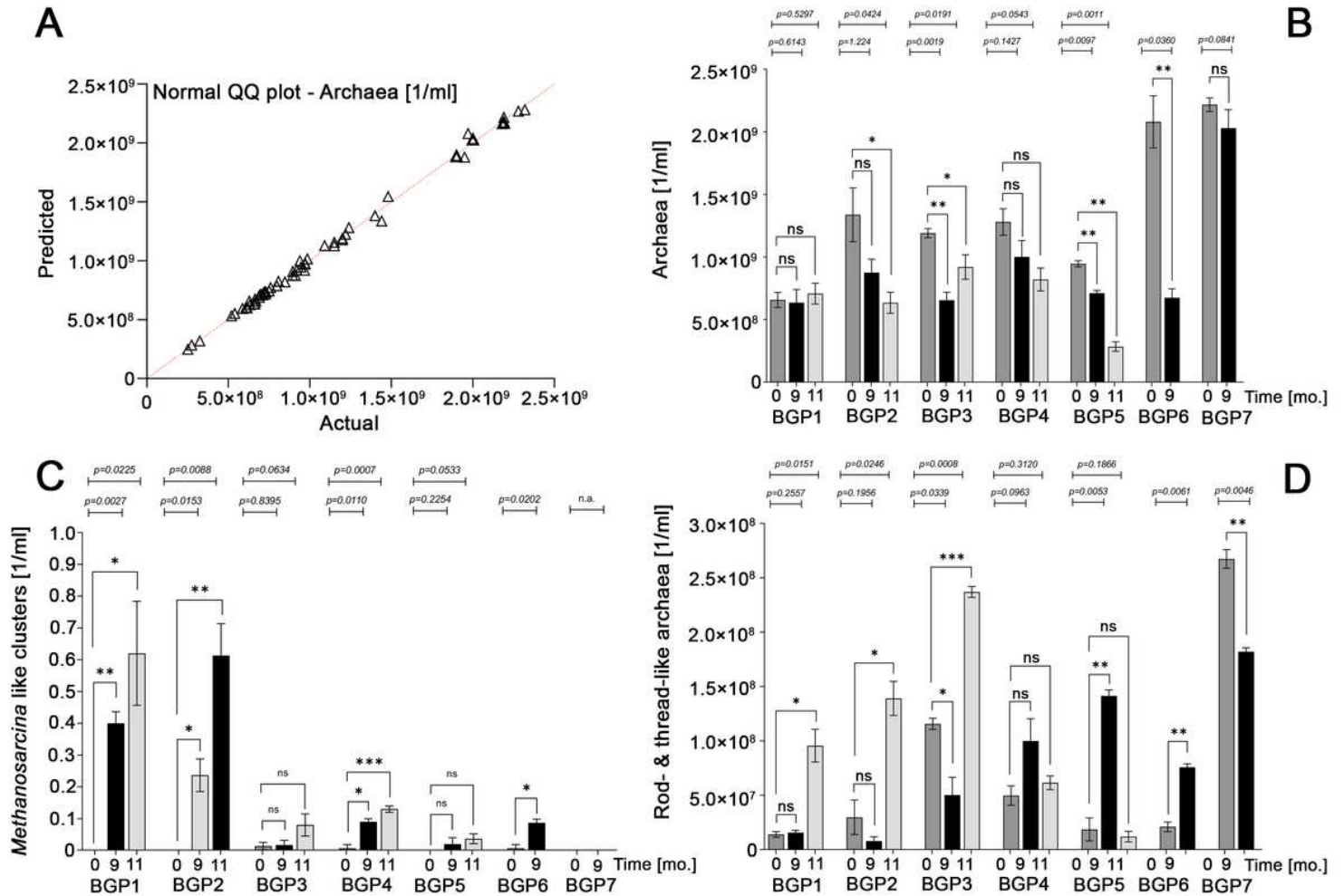


Figure 2

Quantification of methanogenic archaea before and after supplementation: The cofactor F420 was used to count methanogenic archaea using epifluorescent microscopy. The QQ plot resulting from the Shapiro-Wilk test is shown as an example for the counting of all archaea (A), but it was also carried out for the counting of Methanosarcina-like clusters and rod-shaped and thread-like archaea (A). Analysis was performed before biochar was added, and nine and eleven months after supplementation. Each bar shows a mean value of 48 pictures taken from three different slides. (B), Methanosarcina like clusters (C), and rodshaped archaea (D). A two-tailed paired t-test was applied to assess significance.

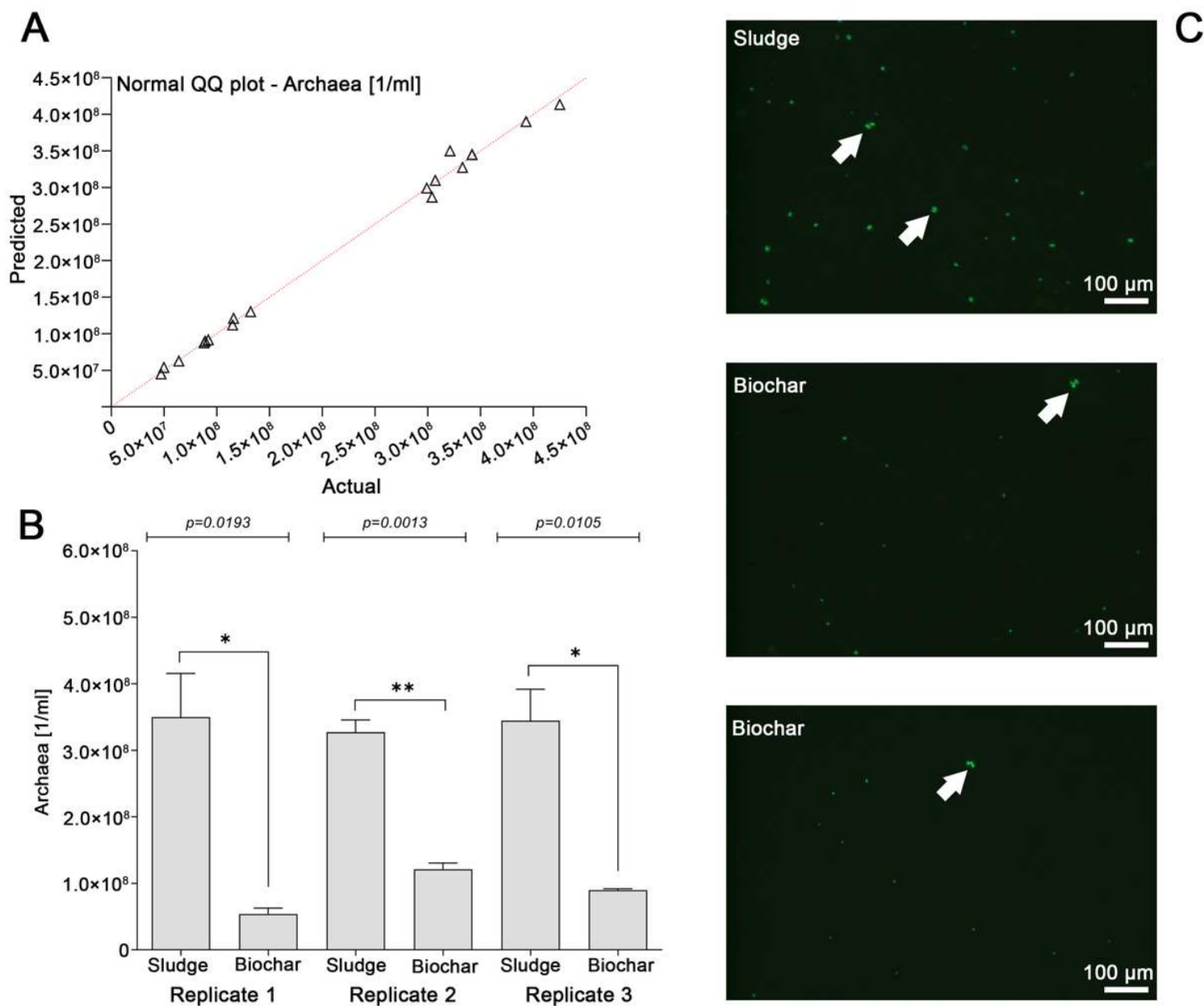


Figure 3

Methanogenic archaea found in biochar particles: After applying the Shapiro Wilk test (A), a two-tailed paired t-test was used to assess significance for all archaea. Number of methanogenic archaea based on the quantification of cofactor F420 signals (B). Biochar particles from BGP1 were collected from the digestate immediately after it left the digester. Pictures of methanogenic archaea found in biochar particles (C). Methanosarcina-like clusters are highlighted with white arrows.

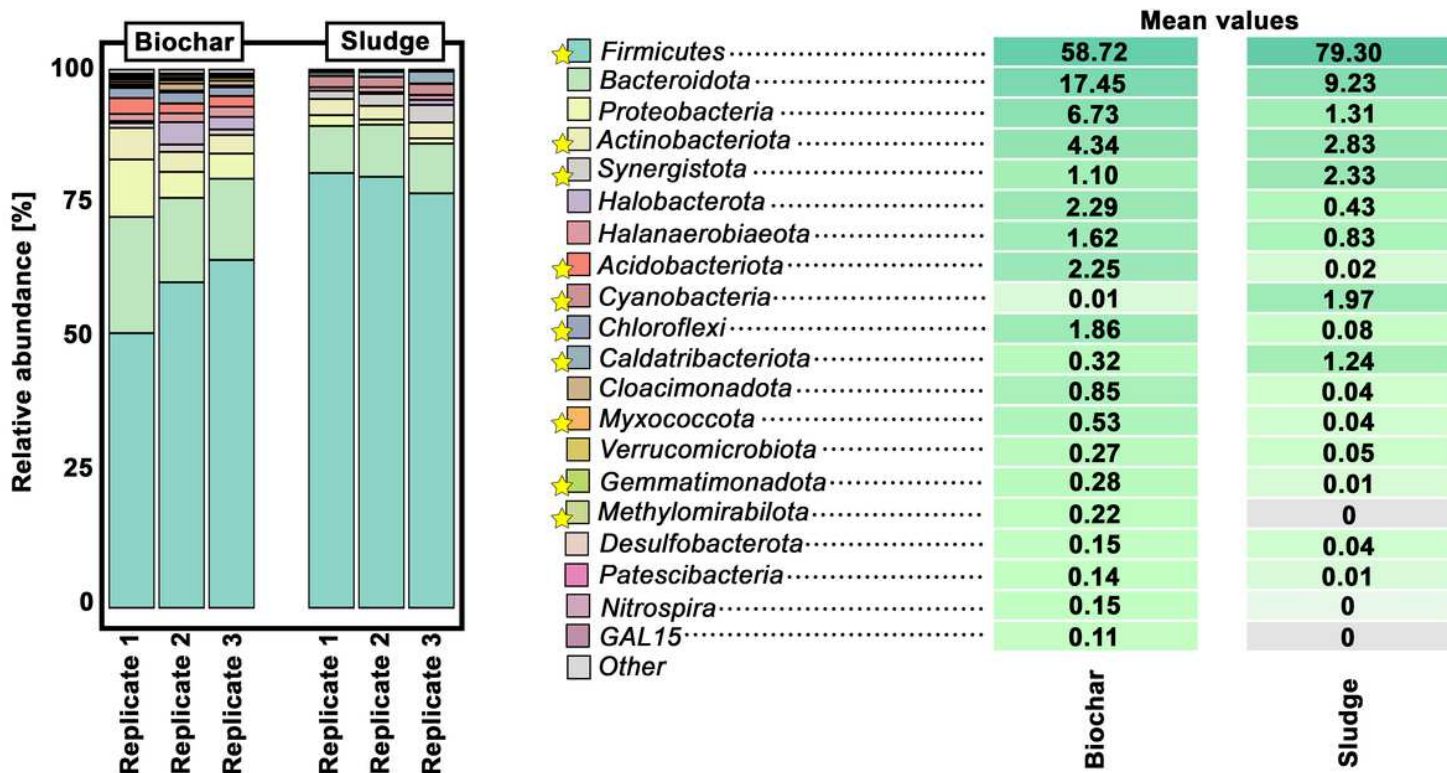


Figure 4

Taxonomic profiles in sludge and biochar from BGP1 at phylum level, obtained through 16S-rRNA gene amplicon high-throughput sequencing. For the sake of simplicity, only the most abundant phyla are shown. Differences in the mean values that are significant are highlighted by yellow stars in the legend. Significances were analyzed using the DESeq2 differential abundance analysis [21] and p-values were < 0.05.

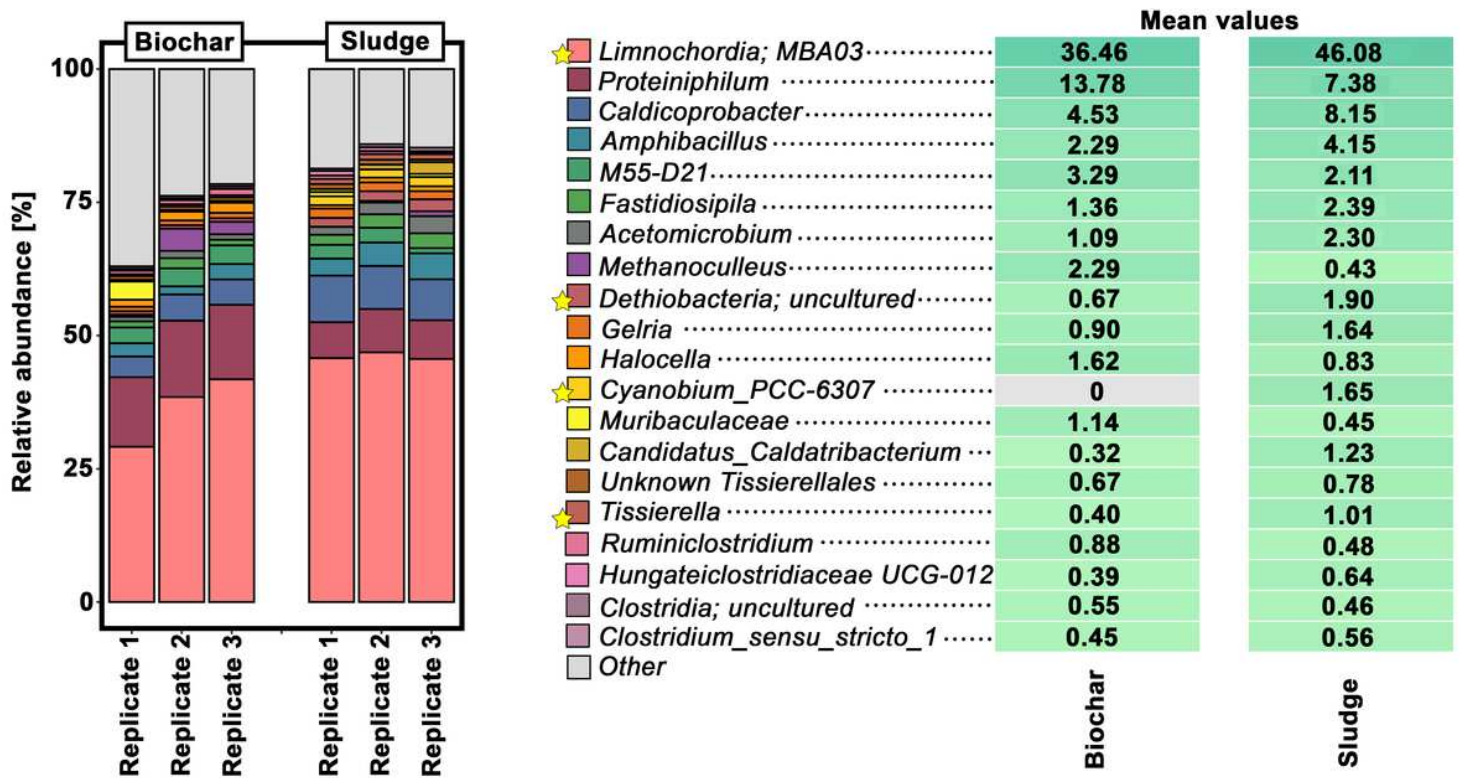


Figure 5

Taxonomic profiles in sludge and biochar from BGP1 at genus level and obtained through 16S-rRNA gene amplicon high-throughput sequencing. For the sake of simplicity, only the most abundant genera are shown. Differences in the mean values that are significant are highlighted by yellow stars in the legend. Significances were analyzed using the DESeq2 differential abundance analysis [21] and p-values were < 0.05.

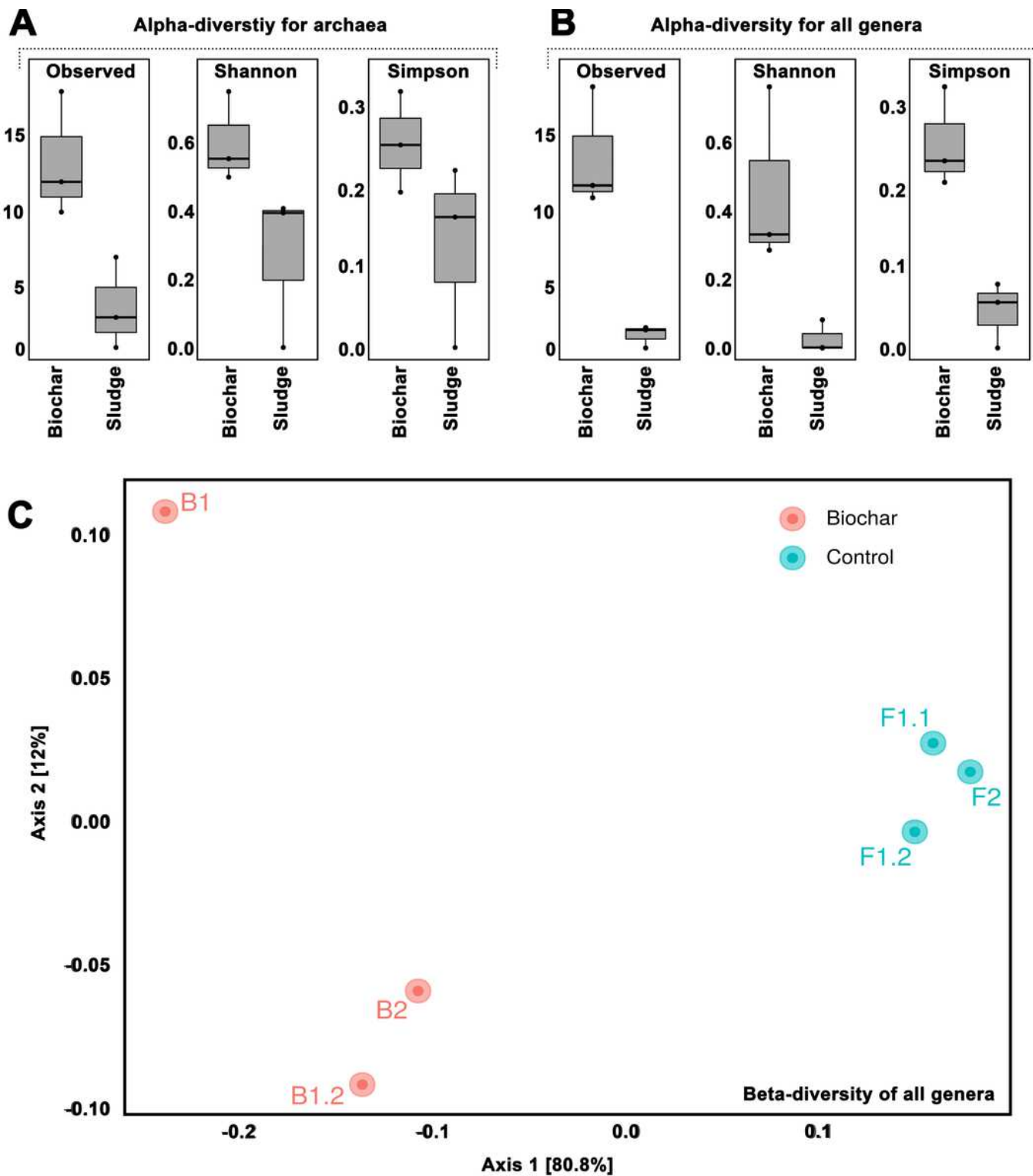


Figure 6

Microbial diversity in biochar particles on genus level: (A) α -diversity of archaea according to richness (Observed) and diversity indices (Shannon and Simpson); (B) α -diversity of all genera according to richness (Observed) and diversity indices (Shannon and Simpson); (C) β -diversity of all genera represented through a Principal Coordinates Analysis.

Supplementary Files

This is a list of supplementary files associated with this preprint. Click to download.

- [Table1.pdf](#)
- [S1.xlsx](#)